

ADVANCES IN FOREST FIRE RESEARCH

2022

Edited by

**DOMINGOS XAVIER VIEGAS
LUÍS MÁRIO RIBEIRO**

Modelling wildfire firebrand accumulation in front of walls perpendicular to the wind

Simona Dossi; Guillermo Rein*

Department of Mechanical Engineering, and Leverhulme Centre for Wildfires, Environment, and Society,
Imperial College London, London, UK, {g.rein@imperial.ac.uk}

*Corresponding author

Keywords

Embers, Firebrands, WUI, ignition, building damage, safety, accumulation

Abstract

Windblown embers, also known as firebrands, can be generated in large numbers during wildfires and ignite fuels as far as kilometers away from their origin. Firebrands are often cited as the leading cause of building wildfire ignition in the wildland-urban interface. Building ignition via firebrands can occur directly, by landing on or inside the building, or indirectly, by igniting adjacent fuel and creating adjacent flame exposure. Studies have investigated firebrands generation from various fuels, wind-driven transport, and ignition mechanisms on different materials and building features. Less research has been conducted on how firebrands deposit and accumulate around buildings; this knowledge is critical in designing buildings safer to firebrand ignition. Here, we address this need and computationally investigate firebrand landing and accumulation in front of obstacles. We present work on a computational fluid dynamic Fire Dynamics Simulator (FDS) model simulating the published experimental data by Suzuki and Manzello measuring the firebrand accumulation region in front of a vertical wall under firebrand exposure generated by the NIST Dragon and varying wind speeds (4, 6, 8, and 10 m/s) (Suzuki and Manzello, 2017). The simulated firebrand accumulation areas in front of the wall are compared to the experimental observations. The wall obstacle dimensions and wind speeds are varied; and the accumulation patterns and sizes are studied to define the critical design parameters affecting firebrand accumulation. Here we present the current progress, simulation results, and future vision for this research project.

1. Introduction

Wildfires pose a significant risk to life and property, and can cause extensive damage to residential communities. Understanding how wildfire spreads is crucial to mitigate this risk. There are three main wildfire spread pathways: flame radiation, direct flame contact, and firebrand ignition. Embers more generally describe small and hot carbon-based fuel particles; firebrands specifically describe airborne burning particles, which travel through wind-driven transport (Babrauskas, 2018). The type of fuel, flames, and surrounding conditions impact these particles' size, shape, and burning conditions. When firebrands land, they may ignite the target fuel they have contact with, this process is called spotting and the new ignited fires are called spot fires. Firebrand ignition of spot fires includes numerous sub-processes occurring on various spatial scales. Firebrands are first generated by flaming fuel, then transported in the wind, and lastly land on target fuel, possibly igniting it; these processes are illustrated in figure 1 and figure 2. Here we present Fire Dynamics Simulator (FDS) simulations of firebrand exposure of a simple geometric obstacle, a rectangular wall perpendicular to wind flow, under varying wind speeds and varying wall thicknesses. Results are compared and validated with published experimental results.



Figure 1: Schematic diagram of the five subprocesses of wildfire firebrand building ignition and damage: 1) firebrand generation, 2) wind-driven transport, 3) landing and accumulation, 4) building ignition and 5) fire spread.

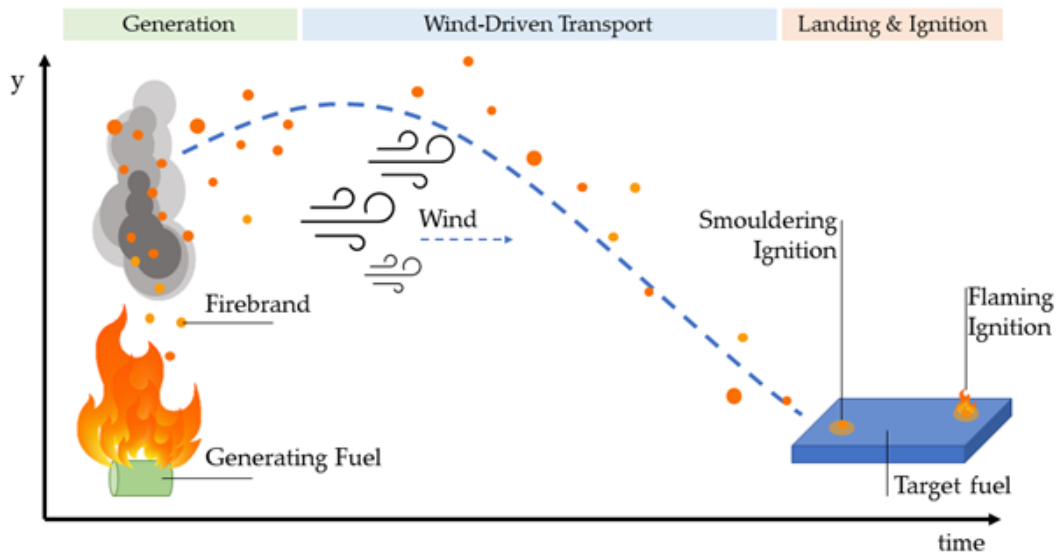


Figure 2: Schematic diagram of firebrand generation, wind-driven transport, and landing and ignition on target fuel, adapted from (Fernandez-Pello, 2017).

1.1. Firebrand Generation and Transport

Firebrands can be generated from a variety of fuels including both vegetative and urban fuel. Extensive research has been produced characterising the firebrand characteristics generated from specific fuels; including Douglas-fir trees (Manzello, Maranghides and Mell, 2007), full scale burning buildings (Suzuki et al., 2012), different roof materials and designs (Waterman, 1969), prescribed fires (El Houssami et al., 2016; Filkov et al., 2017) and actual wildland-urban interface fires (Manzello and Foote, 2014). Figure 3 is a photograph from the 2018 Delta fire in California, and shows the high number of firebrands which can be produced under certain wildfire conditions. Characterisation parameters include, mass and size distribution of firebrands, number of firebrands, projected area of landed firebrands; researchers stress the need for more data of firebrand characterisations from real wildfires and wildland-urban interface fires. The physical firebrand characteristics impact the forces acting on them during wind-driven transport, and therefore their trajectory; their physical and chemical characteristics, and initial conditions determine the type of combustion.



Figure 3: Firebrand shower during the 2018 Delta Fire in the Shasta-Trinity National Forest, California, USA. Photo courtesy of Noah Berger/Associated Press (noahbergerphoto.com). Photo shows numerous airborne firebrands and flames on the grass appears to be ignited by the landing firebrands

Models describing the breakage of firebrands during generation have been developed; Barr and Ezekoye used simple mechanical breakage models coupled with thermal decomposition model which predicts the size distribution of firebrands lofted from a fractal tree which can be combine with plume models to describe the breakage, transport, and mass loss of firebrands in wildfire conditions (Barr and Ezekoye, 2013). Tohidi et.al. studied the mechanical response of wooden elements under external loading after having been heated in wildfire conditions to mimic the firebrand breakage fuel during firebrand generation (Tohidi et al., 2017).

The breakage conditions determine the initial position and conditions of the firebrand's wind-driven transport. Extensive research has been conducted in the field of firebrand transport. Transport models calculated the maximum horizontal transport (spotting) distance for different firebrand conditions: firebrand particles lofted by transitory flaming group of trees (Albini, 1979), by the persistent flaming fuel piles (Albini, 1981) by the thermal fields transporting firebrands by the wind field (Albini, 1983).

Sardoy et al. calculated the wind flow trajectories and burning rates of disk-shaped firebrands initially lofted by crown fire plumes for carrying wind speeds and fire intensities (Sardoy et al., 2007). Anthenien et.al created a numerical model describing the burning and wind transport processes for spherical cylindrical, and disk firebrands lofted by fire plumes (Anthenien, Tse and Carlos Fernandez-Pello, 2006). Detailed review papers cover and compare the many firebrand transport and combustion models developed (Koo et al., 2010).

1.2. Firebrand Landing and Ignition

Firebrands can be transported to, and land on vegetative fuel or urban fuel; spot fires can spread wildfire in the wildland and to the wildland-urban interface (WUI) igniting homes and communities. Here we consider the landing and accumulation of firebrand in front of solid obstacles mimicking building components to investigate WUI fire ignition by firebrands. There are three main general pathways for firebrand ignition of buildings:

1. Indirect ignition: firebrands ignite vegetation or combustibles near the building, the flaming fire spreads and ignite the building.
2. Direct ignition - building interior: firebrand enter the building structure through openings and ignite combustibles inside the building.
3. Direct ignition - building exterior: firebrands accumulate on the building exterior and ignite the building exterior material

Experimental research has characterized firebrand ignition conditions of various objects and materials. the NIST dragon is an experimental apparatus which creates a continuous feed of adaptable speed airflow with burning firebrands (Manzello and Suzuki, 2013). The dragon generates firebrands which match the size and mass flux distribution of real wildfire scenarios, thus allowing the experimental investigation of realistic firebrand exposure. The NIST dragon has been used to study the response of many building targets including: roofing assemblies (Manzello et al., 2010), wall sidings and eaves set ups (Manzello, Suzuki and Hayashi, 2012), decking assemblies (Manzello and Suzuki, 2014), fences (Suzuki et al., 2016). IBHS has used an adaption of the dragon to test full scale buildings in a wind tunnel under various conditions.

For a firebrand to be able to ignite spot fires, the firebrands must heat the target fuel to ignition temperature. Studies have investigated the necessary firebrand mass and temperature to ignite various materials including: structural wood (Santamaria et al., 2015), and fuel beds with varying properties, including: water content, vegetation, geographical origin (Hadden et al., 2011)(Viegas et al., 2014)(Urban et al., 2019).

1.3. Modelling Landing and Accumulation

Models calculating firebrand landing locations and distributions considering varying surrounding conditions and firebrand material and combustion properties have been developed. Such models allowed calculation of ground level mass distribution of disk-shaped firebrands for varying fire intensities and wind speeds (Sardoy et al., 2008). To investigate more specifically at firebrand landing patterns near or on buildings, and the various material fire responses possible, requires more detail. Research has started focusing on firebrand landing position and distributions, around solid obstacles resembling building constructions or building components.

Ngyugen investigated the accumulation patterns of particles resembling firebrands on different rooftop designs in wind tunnel experiments and found numerous complex factors, including roof design details, wind speed and wind direction, which determined where and how firebrands land and accumulate on rooftops (Nguyen and Kaye, 2021). Experiments looking at the response and accumulation patterns in front of obstacles and in between

cuboid obstacles representing inter-building distance in the WUI (Butler et al., 2017; Suzuki and Manzello, 2017; Mankame and Shotorban, 2021). Results advance understanding indirect ignition, and direct ignition of building exterior, by increasing insight on where and for how long firebrands are most likely to land under varying conditions and ignite buildings. Firebrand deposition around cubic obstacles has been modeled using Large Eddy Simulations for turbulence and Lagrangian particle tracking for firebrand trajectory (Mankame and Shotorban, 2021).

With the objective of investigating how building design parameters affect the firebrand landing and accumulation around buildings, here we use the Fire Dynamics Simulator (FDS) to model firebrand exposure and ground level distribution with varying windspeeds perpendicular to a vertical wall of varying heights. We model the experimental set up conducted by Suzuki and Manzello in 2017, to compare results and validate this model (Suzuki and Manzello, 2017). By comparing the landing distribution of firebrands with published experimental results, and varying obstacles shapes, we comment on using models to determine the most hazardous designs and conditions for firebrand ignition in wildfire conditions.

2. Methodology

2.1. Simulation parameters

We present FDS simulations mimicking the experimental set up of a published study investigating firebrand accumulation zones in front of walls (Suzuki and Manzello, 2017). In the experiment, Douglas-fir wood firebrands are fed continuously toward a wall 7.5 m away, perpendicular to feed. The wind tunnel speed and the wall dimensions are varied to test the effect on firebrand accumulation pattern in front of the wall. The experimental set up is shown in figure 4 by a schematic diagram and photos from (Suzuki and Manzello, 2017). The area of the firebrand accumulation piles, and the distance between the pile and the wall were measured and presented. Different FDS computational domain dimensions were tested in order to minimize computational resources, without compromising result accuracy. Figure 5 presents a schematic and screenshot of the final FDS computational domain dimensions. Table 1 compares the properties of the firebrands, wind flow, and wall obstacle in the experimental investigation, and in the FDS simulation.

The wind profile, and firebrand positions are calculated by FDS, and MATLAB image analysis is used to calculate the accumulated area of firebrands. The wall size and shape is varied as in the experimental investigation: sizes 2.4 m x 2.4 m and 1.3 m x 2.4 m were first simulated. The wind speed was also varied as in the experimental investigation; wind speeds 4, 6, 8, and 10 m/s are considered. Simulations with varying wall length and width, and additional solid obstacles will be conducted when the model is validated.

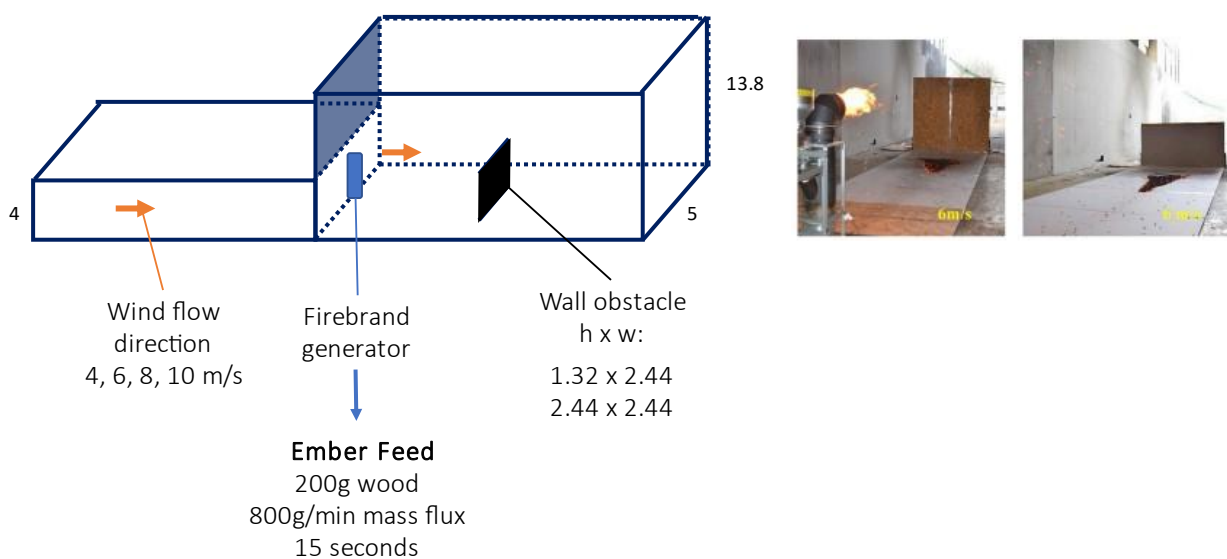


Figure 4: (left): Schematic of wind tunnel, with dimensions in meters, and experimental set up (right:) Photos of experimental set up from (Suzuki and Manzello, 2017)

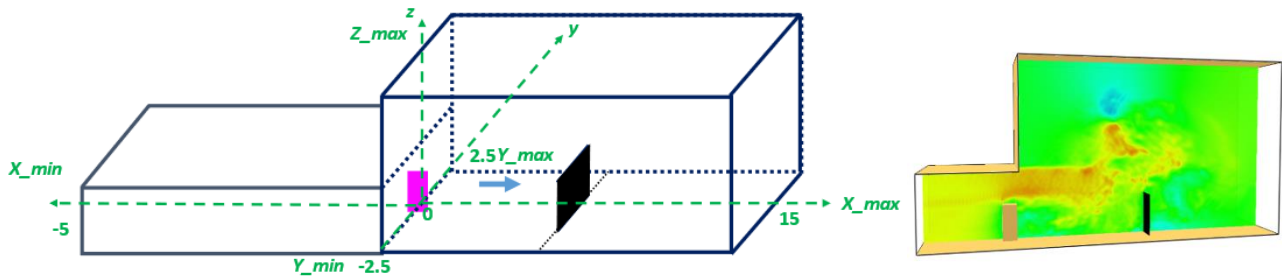


Figure 5: (left): Schematic of FDS computational domain (right:) FDS computational domain with wind speed of 4 m/s at y=0 and t=5 seconds

Table 1: Properties and parameters of the firebrand particles, wind speed, and walls, tested in the experimental investigation, and simulated in this FDS simulation

| | Experiment: (Suzuki and Manzello, 2017) | FDS simulation |
|---|--|--|
| Firebrand [Size, shape, mass flux, material] | 7.9 mm x 7.9 mm x 12.7 mm Cuboid 17.1 g/m ² s Douglas-fir wood | D = 8 mm, L = 13.5 mm Cylindrical 17 g/m ² s Includes particles with both wood and char densities to simulate range of possible particle weights (further physical and chemical properties are defined in model) |
| Wind speed | 4 m/s, 6m/s, 8m/s, 10m/s | 4 m/s, 6m/s, 8m/s, 10m/s |
| Wall [Size] | 2.44 m x 2.44 m 1.32 m x 2.44 m | 2.4 m x 2.4 m 1.3 m x 2.4 m |

2.2. Particle Tracking and Turbulence Model

FDS uses Lagrangian particle tracking to calculate particle position and trajectory in the computational domain, and Large Eddy Simulation (LES) to calculate turbulent flow. By default firebrand particles are modelled as cylindrical particles. Simulated particles do not experience thermal degradation, to mitigate this limitation particles with both unburned wood densities, and wooden char densities are introduced to simulate a spectrum of possible particle densities. Lagrangian Particle Tracking method computes a force balance on each singular particle based on Newton's second Law, given in Equation 1. The momentum transferred from particles to surrounding gas is calculated in FDS by Equation 2; and the acceleration of the particles is solved via Equation 3. Where m_p is the particle mass, u_p is the particle velocity, f_b is the momentum transferred from particles to gas, ρ_f is the fluid density, C_D is the drag coefficient, u_f is the fluid velocity, ρ_p is the particle density, A_p is the particle surface area, g is the gravitational constant and V_p is the particle volume.

$$m_p \frac{du_p}{dt} = F_{drag} + F_{bouyancy} + F_{other} \quad (1)$$

$$f_b = \frac{1}{V} \sum [\frac{\rho}{2} C_d A_{pc} (u_p - u_f) |u_p - u_f| - \frac{dm_p}{dt} (u_p - u_f)] \quad (2)$$

$$\frac{du_p}{dt} = g - \frac{\frac{1}{2}(\rho C_d A_{pc})}{m_p} (u_p - u_f) |u_p - u_f| \quad (3)$$

In FDS, turbulence is calculated with LES, with the default Deardoff model. The default near-wall model in FDS uses Wall-Adapting Local Eddy-viscosity model. All solid boundaries are set to have no slip conditions, and wind is introduced and exited in the domain via open boundary conditions.

3. Results

The modeling and data analysis of this project is ongoing. This section current results and explains the result objectives for future work.

3.1. Firebrand Accumulation Distribution

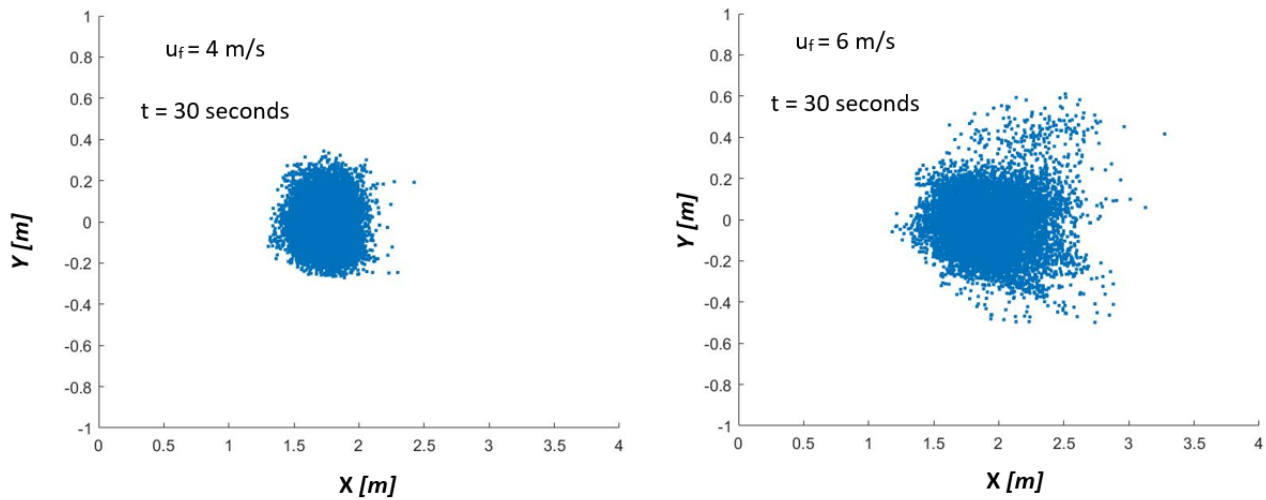


Figure 6: Particle distribution on the floor ($z = 0$) after 15 seconds of firebrand exposure under 4 m/s wind (left) and 6 m/s wind (right).

Figure 6 presents the particle distribution on the floor ($z = 0$) after 15 seconds of firebrand exposure under 4 m/s wind, and 6 m/s wind produced in the FDS simulations. These results show that the accumulated area increases as the wind speed increases, this is the opposite trend presented in (Suzuki and Manzello, 2017). Authors are investigating which parameters are determining this disagreement in simulation results, and experimental observations; especially focusing on the solid boundary conditions of the computational domain, and the particle geometry and related drag coefficient – which have been simplified in the simulation to conserve computational resources.

3.2. Separation Distance

The distance between the firebrand accumulation zone, where firebrands land and stop moving, and the side of the wall facing the firebrand feed is measured in both the experimental investigation, and in the FDS simulations computed. For the FDS simulations, the separation distance is calculated from the final firebrand particle positions at the end of the simulations; these are graphed for each particle in for wind speed of 4 m/s and 6 m/s in figure 7. For a wind speed of 4 m/s the separation distance ranges from 5.1m to 6.2m, for 6 m/s wind the separation distance ranges from 4.2 m to 6.2m. These distances greatly overestimate the separation distances reported in (Suzuki and Manzello, 2017). Furthermore, FDS inaccurately the trend direction of changing separation distance for changing wind speed: experimental measurement confirm that separation distances increase as the wind speed increases, while FDS calculates the opposite trend.

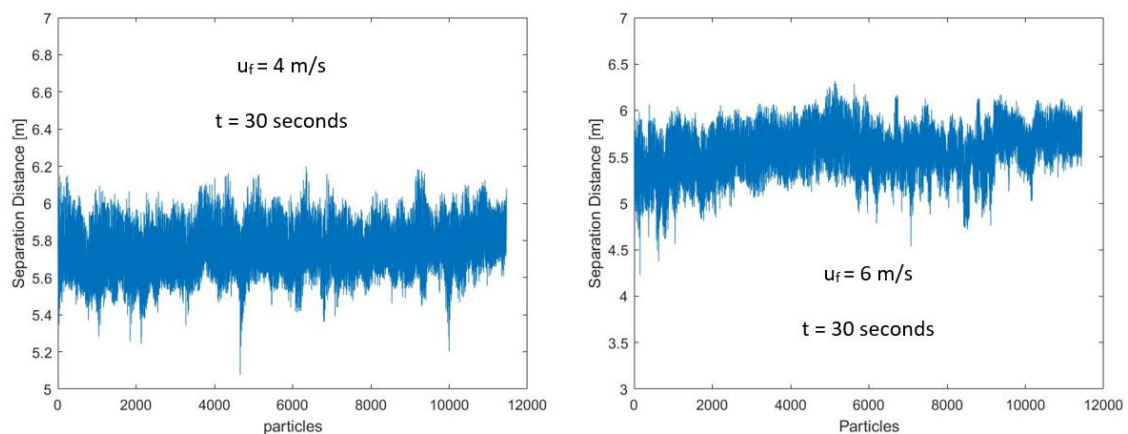


Figure 7: Separation distances between all particles at the end of the simulation ($t = 30$ seconds, after 15 seconds of firebrand exposure) and wall obstacle (located at $x = 7.5$ m), for 4 m/s wind (left) and 6 m/s wind (right).

3.3. Upcoming Work

MATLAB image analysis is being conducted to calculate the projected area of firebrands that have landed and accumulated at $z = 0$ in front of varying obstacles. Numerous simulations varying significant parameters are being carefully analysed to conclude the most significant parameters to simulate firebrand accumulation. Especially, changes to the wind profile simulated in the wind tunnel, and more accurate firebrand particle geometries and drag coefficients are being studied to improve model accuracy.

If the model can be successfully validated with experimental measurements, it will be used to study the building design significance in affecting firebrand accumulation patterns. By varying the wall dimensions, and adding additional solid obstacles to the simulation, the impact of varying building design on firebrand exposure (separation distances, projected area, mass accumulation profile) will be presented. Studying the impact of design considerations on the landing distribution of firebrands in front of walls and sidings is important in designing wildfire resistant WUI buildings and communities.

4. References

- Albini, F. A. (1979) Spot Fire Distance from Burning Trees: A Predictive Model. Edited by U. Intermountain Forest and Range Experiment Station (Ogden. USDA, Forest Service (General technical report INT).
- Albini, F. A. (1981) 'Spot fire distance from isolated sources - extensions of a predictive model', USDA Forest Service Research Note, INT-309, p. 9p.
- Albini, F. A. (1983) 'Transport of firebrands by line thermalst', *Combustion Science and Technology*, 32(5–6), pp. 277–288. doi: 10.1080/00102208308923662.
- Anthenien, R. A., Tse, S. D. and Carlos Fernandez-Pello, A. (2006) 'On the trajectories of embers initially elevated or lofted by small scale ground fire plumes in high winds', *Fire Safety Journal*, 41(5), pp. 349–363. doi: 10.1016/j.firesaf.2006.01.005.
- Babrauskas, V. (2018) 'Firebrands and Embers', in Manzello, S. L. (ed.) *Encyclopedia of Wildfires and Wildland-Urban Interface (WUI) Fires*. Cham: Springer International Publishing, pp. 1–14. doi: 10.1007/978-3-319-51727-8_3-1.
- Barr, B. W. and Ezekoye, O. A. (2013) 'Thermo-mechanical modeling of firebrand breakage on a fractal tree', *Proceedings of the Combustion Institute*, 34(2), pp. 2649–2656. doi: 10.1016/j.proci.2012.07.066.
- Butler, K. M. et al. (2017) 'Wind effects on flame spread and ember spotting near a structure', *15th International Conference and Exhibition on Fire and Materials 2017*, 2, pp. 681–693.
- Fernandez-Pello, A. C. (2017) 'Wildland fire spot ignition by sparks and firebrands', *Fire Safety Journal*, 91(May), pp. 2–10. doi: 10.1016/j.firesaf.2017.04.040.
- Filkov, A. et al. (2017) 'Investigation of firebrand production during prescribed fires conducted in a pine forest', *Proceedings of the Combustion Institute*, 36(2), pp. 3263–3270. doi: 10.1016/j.proci.2016.06.125.
- Hadden, R. M. et al. (2011) 'Ignition of Combustible Fuel Beds by Hot Particles: An Experimental and Theoretical Study', *Fire Technology*, 47(2), pp. 341–355. doi: 10.1007/s10694-010-0181-x.
- El Houssami, M. et al. (2016) 'Experimental Procedures Characterising Firebrand Generation in Wildland Fires', *Fire Technology*, 52(3), pp. 731–751. doi: 10.1007/s10694-015-0492-z.
- Koo, E. et al. (2010) 'Firebrands and spotting ignition in large-scale fires', *International Journal of Wildland Fire*, 19(7), pp. 818–843. doi: 10.1071/WF07119.
- Mankame, A. and Shotorban, B. (2021) 'Deposition Characteristics of Firebrands on and Around Rectangular Cubic Structures', *Frontiers in Mechanical Engineering*, 7(June), pp. 1–14. doi: 10.3389/fmech.2021.640979.
- Manzello, S. L. et al. (2010) 'Quantifying the vulnerabilities of ceramic tile roofing assemblies to ignition during a firebrand attack', *Fire Safety Journal*, 45(1), pp. 35–43. doi: 10.1016/j.firesaf.2009.09.002.
- Manzello, S. L. and Foote, E. I. D. (2014) 'Characterizing Firebrand Exposure from Wildland-Urban Interface (WUI) Fires: Results from the 2007 Angora Fire', *Fire Technology*, 50(1), pp. 105–124. doi: 10.1007/s10694-012-0295-4.
- Manzello, S. L., Maranghides, A. and Mell, W. E. (2007) 'Firebrand generation from burning vegetation', *International Journal of Wildland Fire*, 16(4), pp. 458–462. doi: 10.1071/WF06079.

- Manzello, S. L. and Suzuki, S. (2013) 'Experimentally simulating wind driven firebrand showers in wildland-urban interface (WUI) fires: Overview of the NIST firebrand generator (NIST dragon) technology', *Procedia Engineering*, 62, pp. 91–102. doi: 10.1016/j.proeng.2013.08.047.
- Manzello, S. L. and Suzuki, S. (2014) 'Exposing decking assemblies to continuous wind-driven firebrand showers', *Fire Safety Science*, 11, pp. 1339–1352. doi: 10.3801/IAFSS.FSS.11-1339.
- Manzello, S. L., Suzuki, S. and Hayashi, Y. (2012) 'Exposing siding treatments, walls fitted with eaves, and glazing assemblies to firebrand showers', *Fire Safety Journal*, 50, pp. 25–34. doi: 10.1016/j.firesaf.2012.01.006.
- Nguyen, D. and Kaye, N. B. (2021) 'Experimental investigation of rooftop hotspots during wildfire ember storms', *Fire Safety Journal*, 125(August), p. 103445. doi: 10.1016/j.firesaf.2021.103445.
- Santamaria, S. et al. (2015) 'Investigation of Structural Wood Ignition By Firebrand Accumulation', *The First International Conference on Structural Safety under Fire and Blast*, (July 2016), pp. 1–13.
- Sardoy, N. et al. (2007) 'Modeling transport and combustion of firebrands from burning trees', *Combustion and Flame*, 150(3), pp. 151–169. doi: 10.1016/j.combustflame.2007.04.008.
- Sardoy, N. et al. (2008) 'Numerical study of ground-level distribution of firebrands generated by line fires', *Combustion and Flame*, 154(3), pp. 478–488. doi: 10.1016/j.combustflame.2008.05.006.
- Song, J. et al. (2017) 'The Wind Effect on the Transport and Burning of Firebrands', *Fire Technology*, 53(4), pp. 1555–1568. doi: 10.1007/s10694-017-0647-1.
- Suzuki, S. et al. (2012) 'Firebrand generation data obtained from a full-scale structure burn', *International Journal of Wildland Fire*, 21(8), pp. 961–968. doi: 10.1071/WF11133.
- Suzuki, S. et al. (2016) 'Ignition of Wood Fencing Assemblies Exposed to Continuous Wind-Driven Firebrand Showers', *Fire Technology*, 52(4), pp. 1051–1067. doi: 10.1007/s10694-015-0520-z.
- Suzuki, S. and Manzello, S. L. (2017) 'Experimental investigation of firebrand accumulation zones in front of obstacles', *Fire Safety Journal*, 94(April), pp. 1–7. doi: 10.1016/j.firesaf.2017.08.007.
- Tohidi, A. et al. (2017) 'Thermo-mechanical breakage mechanism of firebrands', *10th U.S. National Combustion Meeting*, 2017-April(April).
- Urban, J. L. et al. (2019) 'Ignition of a spot smolder in a moist fuel bed by a firebrand', *Fire Safety Journal*, 108(May), p. 102833. doi: 10.1016/j.firesaf.2019.102833.
- Viegas, D. X. et al. (2014) 'Ignition of Mediterranean Fuel Beds by Several Types of Firebrands', *Fire Technology*, 50(1), pp. 61–77. doi: 10.1007/s10694-012-0267-8.
- Waterman, T. E. (1969) *Experimental Study of Firebrand Generation*. Chicago. Available at: <https://apps.dtic.mil/sti/pdfs/AD0695640.pdf>.